Experimental Study on Helium-Air Exchange Flow Through Small Openings with Vertical Partition

Tae-il Kang*

(*Received February 2, 1998*)

The helium-air exchange flow may occur at the rupture accident of a standpipe in a high temperature engineering test reactor. A test vessel with three types of small opening is used for experiments. An estimation method of mass increment is applied to measure the exchange flow rate. Flow measurements are made with the single opening and partitioned opening, for opening ratios H_1/D_1 in the range 0.05 to 10, where H_1 and D_1 are height and diameter of the opening, respectively. At lower opening ratios ($H_1/D_1<0.75$), the difference in the exchange flow rates between the opening systems is small. At higher opening ratios ($H_1/D_1 \geqq 0.75$), exchange flow rates of the partitioned opening system are higher than those of the single opening system because of separated (unidirectional) flows by partition. An effect of variation of diameters of the partitioned openings on the exchange flow rate is investigated. The exchange flow rate increases with the opening diameter. Finally, an experiment with two-opening is designed to investigate the effect of fluid interaction of the partitioned opening system. It is demonstrated that the exchange flow rate of the two-opening system is higher than that of the partitioned opening system because of the absence of the fluid interaction.

Key Words: HTTR (High Temperature Engineering Test Reactor), Exchange Flow, Partition, Fluids Interaction, Mach-Zehnder Interferometer

Nomenclature

D_1 : Diameter of opening (m)
D_f : Effective diameter of opening (m)
F_r : Froude number
g : Aacceleration due to gravity (m/s^2)
H_1 : Height of opening (m)
m_{He} : Mass of helium (kg)
mL : Mass of gas mixture (kg)
Δm : Mass increment (kg)
Q : Volume exchange flow rate (m^3/s)
t : Time (s)
V : Volume of test vessel (m^3)
δ : Partition thickness (m)
ρ : Density (kg/m^3)
ρ_m : Mean density $=(\rho_H+\rho_L)/2$ (kg/m^3)
$\Delta\rho_L$: Density increment (kg/m^3)

Subscripts

H : Air
L : Gas mixture
t : Time
0 : Initial condition

* Department of Architectural Equipment Chang Shin College, 541, Bongam-Dong, Masan, 630-764, Korea

1. Introduction

A high temperature engineering test reactor (HTTR), a small-scale high temperature gas cooled reactor (HTGR), is now being constructed in Japan Atomic Energy Research Institute (JAERI) to establish and upgrade HTGR technologies (JAERI, 1992; Hishida and Fumizawa, 1992). In the safety study of the HTGR, a rupture of standpipe at the top of the reactor vessel is considered as one of the most critical design-base accidents. Figure 1 shows a schematic drawing of the air ingress process after the rupture accident of the standpipe and the HTTR is a graphite moderated HTGR of 30 MW thermal power and 950 °C outlet helium coolant temperature. The standpipes are installed at the top of the reactor

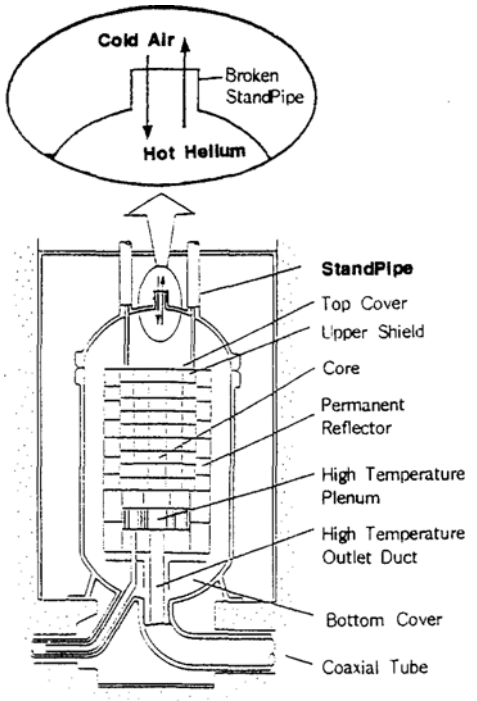

Fig. 1 Schematic diagram of helium-air exchange flow at rupture accident of standpipe in HTTR.

vessel as shown in Fig. 1. When the stand pipes rupture, helium coolant gas in high pressure flows immediately through the breach out of the reactor vessel. After the pressure of the reactor vessel has fallen to that of the atmosphere, the air flows into the reactor vessel, which is caused by buoyancy force due to the density difference between the helium inside the reactor vessel and the air outside. The penetrated air reacts with the high temperature graphite structure, and it causes corrosion of the graphite components, which results in a severe damage of in-core reactor structures. Therefore, it is important to evaluate the penetrated air flow rate during the rupture accident of the standpipe.

From a survey of literature, it appeared that some papers dealt with buoyancy-driven exchange flow with brine-water (Epstein, 1988; Mercer and Thompson, 1975a; Mercer and Thompson, 1975b; Leach and Thompson, 1975) and air-air (Brown and Solvason, 1962a; Brown and Solvason, 1962b). Epstein (1988) made

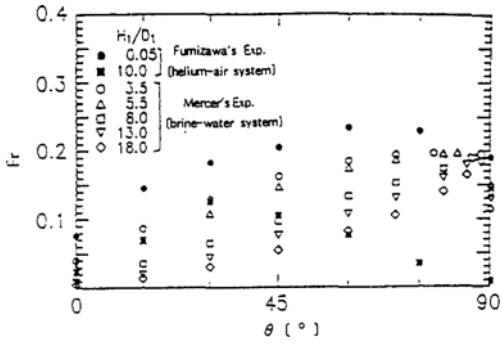

Fig. 2 Relation between Froude number and inclination angle (Fumizawa, 1992).

measurements of the buoyancy-driven exchange flow with a single opening, for opening ratios H_1/D_1 in the range 0.01 to 10, where H_1 and D_1 were the height and the diameter of the opening, respectively. Epstein suggested four different flow regimes, as H_1/D_1 increased through this range. Most of the above studies on the buoyancy-driven exchange flow have been carried out with the single opening and small density difference. However, the density of cold air outside reactor vessel is at least three times larger than that of the gas mixture (helium and hot air) inside reactor vessel at the standpipe rupture accident. Fumizawa (1992) conducted experiments for the helium-air exchange flows with two types of the single opening, vertical and inclined single openings. Fumizawa reported that the experimental results on the helium-air system agreed with those of the Epstein's brine-water system (Epstein, 1998). It was also found that the inclination angle for the maximum Froude number decreased with increasing the opening ratio in the helium-air system, while Mercers's experimental results indicated that the angle remained almost constant in the brine-water system, as shown in Fig. 2 (Fumizawa, 1992).

There were no studies for the exchange flow through the partitioned opening (opening with a vertical partition) previously. In the present study, the single opening is employed to model the rupture of single standpipe and the partitioned opening is employed to model the rupture of multiple standpipes. There are three aims for examining the helium-air exchange flow

through small openings with vertical partition. First, from a fundamental point of view, there is a big difference of flow passages between the partitioned opening and the single opening. Thus, it is necessary to compare the exchange flow rates between the two types of opening. Secondly, effect of various diameters of the partitioned opening on the exchange flow rate is investigated. Finally, effect of fluids interaction of the partitioned opening system on exchange flow rate is discussed.

2. Experimental Apparatus and Procedures

Essential features of the experimental apparatus for the case of three types of opening to evaluate the exchange flow rate are described with aid of Fig. 3. The experimental apparatus is composed of a test vessel, an electronic balance, and a personal computer for data acquisition. The test vessel consists of a test cylinder and opening made from plexiglass. The three types of the opening are employed in the experiments, as shown in Fig. 3. Geometric configurations of the single and the partitioned openings are shown in Fig. 4. A vertical partition of rectangular plate is in alignment with center line of the partitioned opening, where partition thickness δ is 0.5 mm. Seven round openings are fabricated from tubes, and one round opening is hole cut in upper plate of the test cylinder. The opening height H_1 varies from 0.01 to 0.2 m and the opening diameter, D_1, is 0.02 m. The diameter of the test cylinder D_2, is 0.194 m and the height H_2 is 0.4 m. Table 1 describes the sizes of openings and test cylinders to investigate the effect of variation of the opening diameters on the exchange flow rate in the partitioned opening system. Figure 5 shows the test section for investigating the effect of fluids interaction of the partitioned opening system on the exchange flow rate. Each opening is separated by the vertical partition. A distance (0.1 m) between

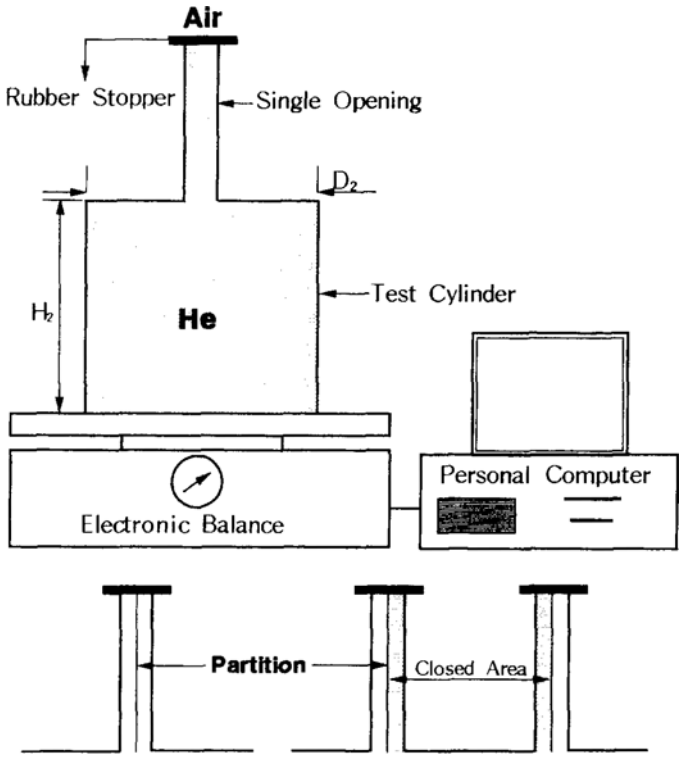

Fig. 3 Schematic diagram of experimental apparatus.

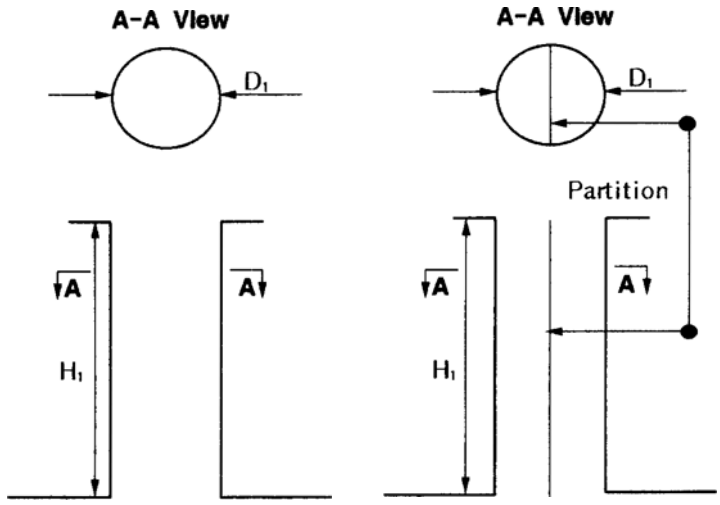

(a) Single opening (b) Partitioned opening

Fig. 4 Schematic diagram of single opening and partitioned opening.

Table 1 Test vessel geometry to investigate effect of opening diameter on exchange flow rate in partitioned opening system.

No.	D_1 m	D_2 m	H_2 m	H_1/D_1
1	0.01	0.1	0.2	
2	0.02	0.194	0.4	2, 10
3	0.04	0.499	0.5	

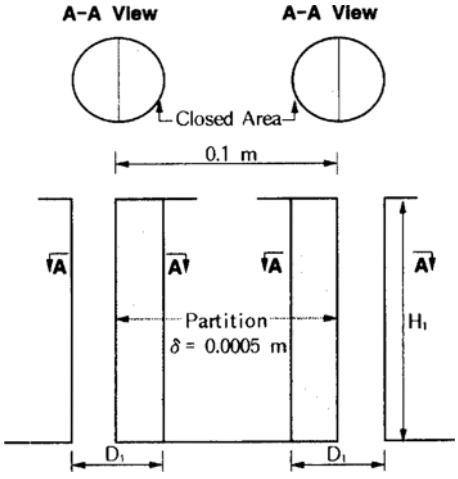

Fig. 5 Schematic diagram of two-opening.

two openings is long enough to remove the fluids interaction between the upward flow of the helium and the downward flow of the air. One

Table 2 Test vessel geometry to investigate effect of fluids interation on exchange flow rate in partitioned opening system.

Opening Type	D_1 m	H_1 m	D_2 m	H_2 m
Partitioned Opening	0.01	0.1	0.1	0.2
Two-Opening	0.01	0.1	0.194	0.4

side of each opening is closed to avoid the fluids interaction. The diameters and heights of the openings and the test cylinders are described in Table 2. A method of mass increment was used to measure the exchange flow rate. The experiments were carried out under the atmospheric pressure and room temperature. The test vessel was filled with pure helium gas initially. The opening's top was sealed with a thin rubber stopper, as shown in Fig. 3. On removal of the rubber stopper placed on the top of the opening, the buoyancy -driven exchange flow was initiated and the heavier air was introduced into the test vessel. Thus, the mass of gas mixture in the test vessel increased. Figure 6 shows optical components of Mach-Zehnder interferometer to visualize the exchange flow. The illumination beam (He-Ne laser supplied from light source, wave length 633 nm) collimated by lens 2 is split by the beam splitter 1 inclined at 45° into a test beam and a

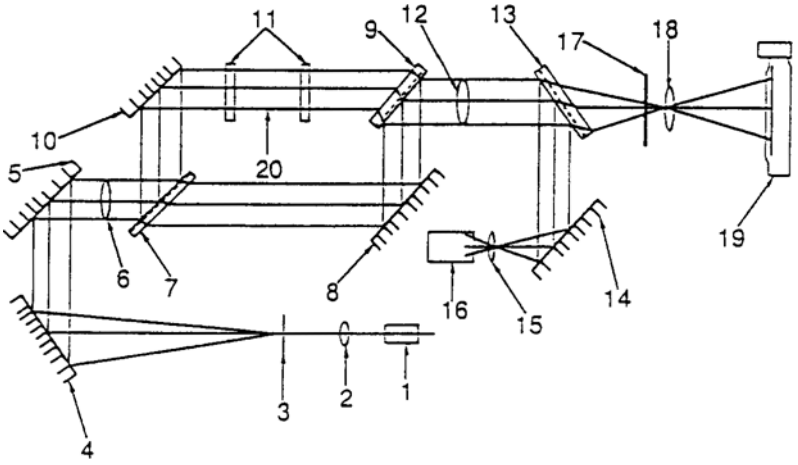

1. Laser 2. Lens 1 3. Pinhole 4. Mirror 1 5. Mirror 2 6. Lens 2 7. Splitter 1
8. Mirror 3 9. Splitter 2 10. Mirror 4 11. Window 12. Lens 3 13. Splitter 3 14. Mirror 5
15. Lens4 16. CCD Camera 17. Screen 18. Lens5 19. 35mm Camera 20. Test Section

Fig. 6 Optical components of Mach-Zehnder interferometer.

reference beam. The test beam reflected by coated surface of the beam splitter 1 is reflected by mirror 4 in order to cross the test section closed by windows. The beam is then transmitted through the beam splitter 2, forming a test section image on observation screen. At the same time, the reference beam transmitted through the beam splitter 1 is successively reflected by mirror 3 and coated surface splitter 2 before being superimposed on the test beam. The beam splitter 2 imposes the same optical path delay on the test beam that the beam splitter 1 does on the reference one. Consequently, the test beam and the reference beam are mixed beyond the beam splitter 2. The test beam and the reference beam interfere, and interference fringe pattern appears on the screen. If density of the test section is homogeneous, straight parallel equidistant interference fringes appear (Yang, 1989). If it is not homogeneous, distorted interference fringes appear. The experimental procedure of the two-opening system are essentially the same as that described in the foregoing for the single opening system and the partitioned opening system, except that the two rubber stoppers are placed, one in each opening. The flow is initiated by removing each stopper simultaneously. The mass increment Δmt of the gas mixture is measured by means of the electronic balance at regular intervals.

$$\Delta m_t = m_{L,t} - m_{He,0} \tag{1}$$

where $m_{L,t}$ is mass of the gas mixture at time t and $m_{He,0}$ is mass of the helium at zero time. The gas mixture's density increment $\Delta\rho_L$ is calculated from the mass increment, and it is given by

$$\Delta\rho_L = \frac{\Delta m_t}{V} \tag{2}$$

where V is volume of the test vessel. The volumetric exchange flow rate Q through the opening is evaluated by

$$Q = \frac{V}{\rho_H - \rho_L}\frac{d\Delta\rho_L}{dt} \tag{3}$$

where ρ_H and ρ_L are density of the air and density of the gas mixture. The volume exchange flow rate is expressed in the form of Froude number, Fr and is defined as

$$Fr = Q\sqrt{\frac{\rho_m}{D_f^5 g(\rho_H - \rho_L)}} \tag{4}$$

The effective diameter D_f is used in Eq. (4) because the partitioned opening and the two -opening are not round, and given by

$$D_f = \sqrt{\frac{4}{\pi}\left(\frac{\pi D_1^2}{4} - D_1\delta\right)} \tag{5}$$

where D_f is D_1 for the single opening.

3. Results and Discussion

3.1 Single opening and partitioned opening

Figure 7 illustrates variations of the density increments for the single opening system and the partitioned opening system with time. The density increment for both opening systems increases with time. As expressed in Eq. (2), the density of the gas mixture in the test vessel increases because the exchange flow occurs. Finally, it approaches the density difference between the air and the helium. Figure 7 shows that the difference in the density increments between the single opening system and the partitioned opening system, for the opening ratios H_1/D_1 in the range 0.05 to 0.75 is not large. However, a big difference in the density increment is found at H_1/D_1 of 10, which will be discussed in the result of flow visualization shown in Fig. 12. Figure 8 shows the variation of Froude numbers of the partitioned opening system with time. The Froude numbers at H_1/D_1 of 0.05 appear to be constant and also, they are almost constant at H_1/D_1 of 10 before 300 second. This means that the density difference between the air and the gas mixture, buoyancy force, is almost constant. The Froude numbers fluctuate at H_1/D_1 of 0.75. Figure 9 is prepared to illustrate comparison of relationship between the Froude number and the density increment. This figure shows that the Froude numbers are almost constant in the range of $0 \leq \Delta\rho_L \leq 0.5$ kg/m^3 at H_1/D_1 of 0.05 and 10. Therefore, in the present experiment, the Froude numbers in Fig. 10 are defined, as average of the

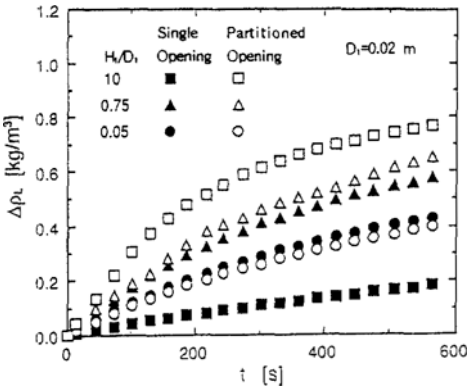

Fig. 7 Comparison of variation of density increment between partitioned opening system and single opening system with time.

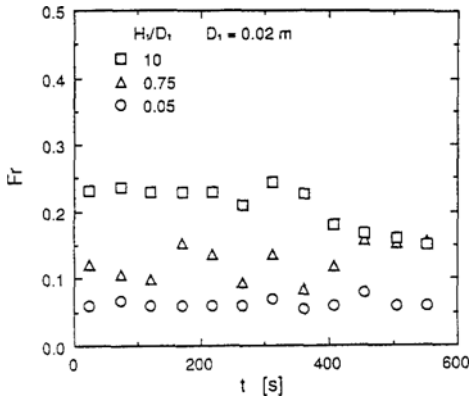

Fig. 8 Variation of Froude number of partitioned opening system with time.

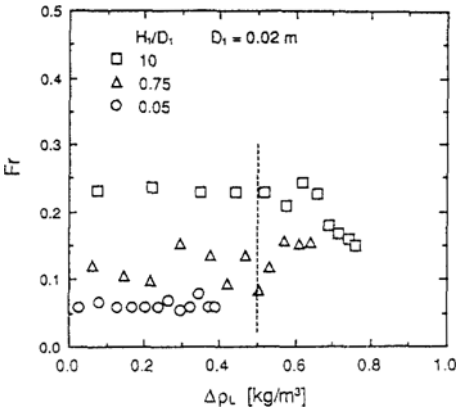

Fig. 9 Varition of Froude number of partitioned opening system with density increment.

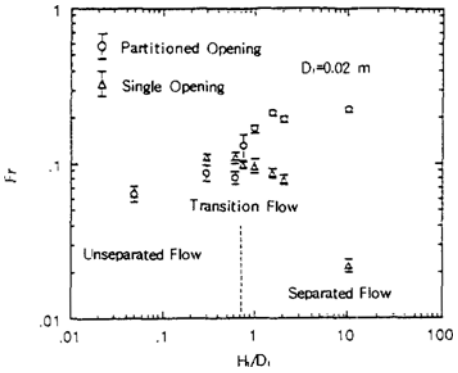

Fig. 10 Comparison of Froude numbers between partitioned opening system and single opening system.

Froude numbers in the range of $0 \leq \Delta\rho_L \leq 0.5$ kg/m^3. In Fig. 10, the exchange flow rate is plotted in the form of the Froude number, as a function of the opening ratio H_1/D_1. For the exchange flow through the single opening with brine and water, Epstein's experimental results were divided into the following exchange flow regimes: (I) oscillatory exchange flow regime, (II) countercurrent Bernoulli flow regime, (III) regime of combined turbulent diffusion and Bernoulli flow, and (IV) turbulent diffusion regime (Epstein, 1988). The present experimental results in the single opening system with the helium and air are also divided into four flow regimes. At lower opening ratios ($H_1/D_1 < 0.75$), difference in the exchange flow rates between the single opening system and the partitioned opening system is small because the upward flow and the downward flow are not separated (bidirectional), as shown in Fig. 11. However, at higher opening ratios ($H_1/D_1 > 0.75$), the exchange flow rates of the partitioned opening system are larger than those for the single opening system. These experimental results indicate that the partition reduces flow resistance at the higher H_1/D_1 because the upward flow of the helium and the downward flow of the air are separated (unidirectional) by the vertical partition within the opening, as shown in Fig. 11. The Froude numbers for the partitioned opening system at H_1/D_1 of 0.75 fluctuate with time, as shown in Fig. 8, and thus, the standard deviation is large, as plotted in Fig. 10. Three flow regimes in the partitioned opening system are divided based on figure 10: (1) unseparated flow regime ($H_1/D_1 < 0.75$), (2) transition flow regime ($H_1/D_1 = 0.75$), (3) separated flow regime ($H_1/D_1 > 0.75$). Figure 12 shows examples of Mach-Zehnder interferograms, and flow patterns are compared. Because distance between the effective plane mirrors of the Mach-Zehnder interferometer is confined, the heights and diameters of the openings are reduced to a half size for flow visualization. The opening diameter is 0.01 m and the opening ratios are 0.05, 0.3, 0.75, 2, and 10. Left figures and right figures in Fig. 12 show flow patterns of the partitioned opening system and the single opening system, respectively. Distorted interference fringes show that the light helium flows out from the opening entrance. The upward flows of helium through the single and the partitioned openings in Fig. 12 swing in lateral direction at $H_1/D_1 < 0.75$. It is observed that the upward flow of helium and the downward flow of the air do not take place stably, because the flows within the single and the partitioned opening are unseparated flows. Thus, they interact strongly with each other at the opening entrance. The unseparated flow increases strength of flow resistance between two fluids and therefore, the exchange flow rates of the partitioned opening system are low, as shown in Fig. 10. The fringes of the upward flow of the helium swing strongly at H_1/D_1 of 0.75 in the partitioned opening system, as shown in Fig. 12, and the Froude numbers shown in Fig 8. fluctuate at H_1/D_1 of 0.75. It is shown that the result of flow visualization agrees with that of flow measurement. Based on the above experimental results, it is judged that the transition flow regime exists at H_1/D_1 of 0.75 in the partitioned opening system. It is clearly visualized that the upward flow of helium and the downward flow of the air in the partitioned opening system take place smoothly and stably in separated flow passages within the partitioned opening at higher H_1/D_1, $H_1/D_1 > 0.75$. Amplitudes of the fringes of the upward flow of the helium in the partitioned opening system are larger than those of the fringes of the upward flow of the helium in the single opening system. The separated flow causes less flow resistance and thus, the exchange flow rate of the partitioned opening system increases with the opening ratio in the separated flow regime. The distorted inter-

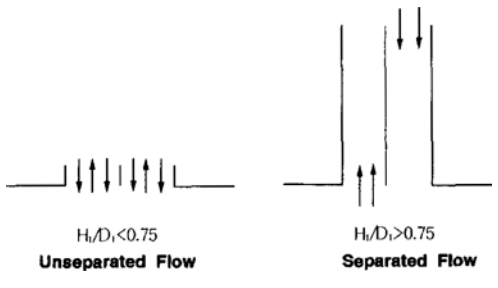

Fig. 11 Schematic view of flow configurations suggested in partitioned opening system.

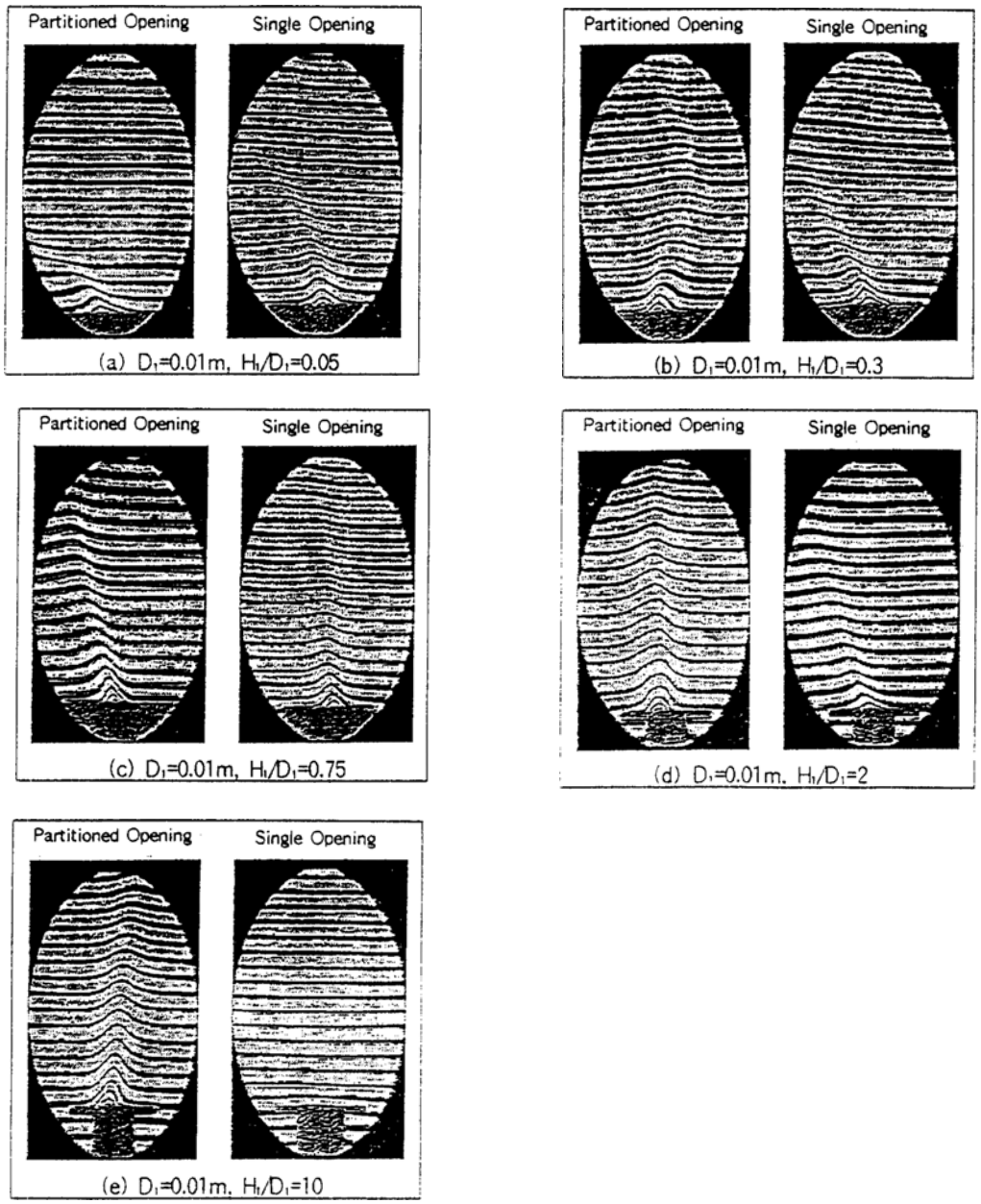

Fig. 12 Comparison of flow visualizations between partitioned opening system and single opening system (t=60 s).

ference fringes of the helium of single opening system shown in Fig. 12 at H_1/D_1 of 10 do not appear because the exchange flow rate shown in Fig. 10 is too low. Flow configurations of the exchange flow in the partitioned opening system are divided into the separated flow and the unseparated flow, as shown in Fig. 11, based on comparison of the exchange flow rates and the Mach-Zehnder interferograms. Effect of variation of opening diameters of the partitioned opening on the exchange flow rate is investigated in separated flow regime ($H_1/D_1>0.75$). The opening diameters are 0.01, 0.02, and 0.04 m, and the opening ratios are 2 and 10. Figure 13 shows the

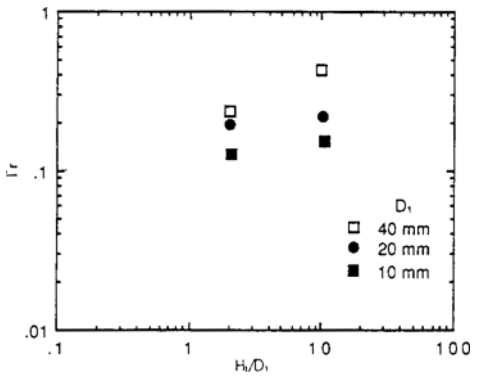

Fig. 13 Comparison of Froude numbers with opening diameter.

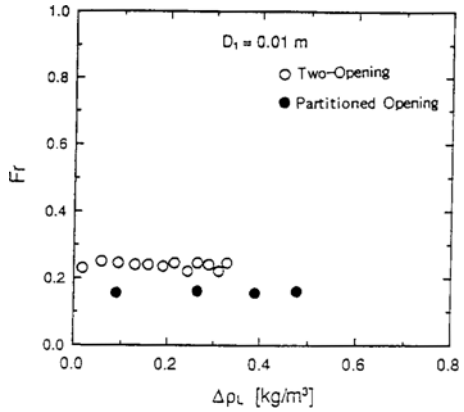

Fig. 14 Comparison of variation of Froude numbers between partitioned opening system and two-opening system with density increment.

Froude numbers with the opening ratios for the opening diameters 0.01, 0.02, and 0.04 m. The Froude numbers increase with the opening diameters because the flow region is the separated flow regime ($H_1/D_1 > 0.75$).

3.2 Two-opening

Figure 14 shows the difference in the Froude numbers between the two-opening system and the partitioned opening system. The difference indicates that the fluid interaction takes place as a flow resistance to the flow exchange. Based on the flow visualizations of Fig. 15, it is clearly shown that amplitudes of the fringes of the upward flow of helium in the two-opening system are larger than those of the fringes of the upward flow of helium in the partitioned opening system. The exchange flow of the two-opening system due to less flow resistance gives rise to the larger amplitudes at the opening entrance. Therefore, the exchange flow rate of the two-opening system is larger than that of the partitioned opening system because of the absence of fluids interaction at the opening entrance, as shown in Table 3.

Table 3 Comparison of Froude numbers between partitioned opening system and two-opening system.

Opening Type	Froude Number
Two-Opening	0.2381
Partioned Opening	0.1571

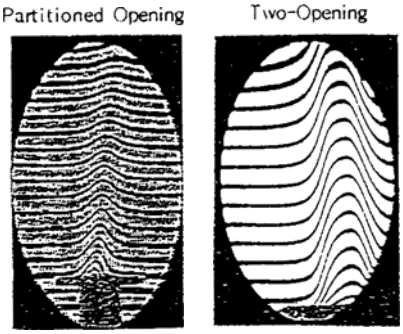

D_1=0.02 m, H_1/D_1=10, t=60 s

Fig. 15 Comparison of flow visualizations between partitioned opening system and two-opening system.

4. Conclusions

An experimental study of the helium-air exchange flows through the small openings has been carried out in order to understand the character of the penetrated air flow at the rupture accident of the standpipe in the HTTR. In this paper, effects of the partition and the fluids interaction on the exchange flow were investigated and discussed experimentally. Further flow visualization will be required to investigate the downward flow of the air within the test cylinder that governs the flow patterns and the exchange flow rates. Conclusions of this paper are summarized in the five groups as follows:

(1) The difference in the exchange flow rates

between the single opening system and the partitioned opening system at the lower opening ratios ($H_1/D_1<0.75$) is small because of the unseparated flow.

(2) The Froude numbers of partitioned opening system are higher than those for the single opening system at the higher opening ratios ($H_1/D_1>0.75$), because of the separated flow.

(3) The Froude number increases with the opening diameter in the separated flow regime.

(4) Based on the flow visualizations by Mach-Zehnder interferometer, it is observed that the amplitudes of the fringes of the upward flow of the helium in the two-opening system are larger than those of the fringes of the upward flow of the helium in the partitioned opening system.

(5) The Froude number of the two-opening system is higher than that of the partitioned opening system because of the absence of the fluid interaction.

Acknowledgments

The author wishes to thank Dr. M. Fumizawa of Japan Atomic Energy Research Institute for a number of useful discussions.

References

Brown, W. G. and Solvason, K. R., 1962a, "Natural convection through Rectangular Openings in Partitions-1," *Int. J. Heat Mass Transfer,* Vol. 5, No. 5, pp. 859~867.

Brown, W. G. and Solvason, K. R., 1962b, "Natural Convection Through Rectangular Openings in Partitions-2," *Int. J. Heat Mass Transfer,* Vol. 5, No. 5, pp. 869~878.

Epstein, M., 1988, "Buoyancy-Driven Exchange Flow Through Small Openings in Horizontal Partitions," *Trans. of ASME,* Vol. 110, pp. 885~893.

Fumizawa, M., 1992, "Experimental Study of Helium-Air Exchange Flow Through a Small Opening," *Kerntechnik,* Vol. 57, No. 3, pp. 156~160.

Hishida, M. and Fumizawa, M., 1992, "Researches on Air Ingress Accidents of HTGR," *Proc. Int. Conf. on Design & Safety of Advanced Nuclear Power Plants,* Tokyo, pp. (18.4-1)~(18.4-7).

JAERI, 1992, "Present Status of HTGR Research and Development," *JAERI.*

Leach, S. J. and Thompson, H., 1975, "An Investigation of Some Aspects of Flow into Gas Cooled Nuclear Reactors Following an Accidental Depressurization," *J. Br. Nucl. Energy Soc.,* Vol. 14, No. 3, pp. 243~250.

Mercer, A. and Thompson, H., 1975a, "The Exchange Flow in Inclined Ducts," *J. Br. Nucl. Energy Soc.,* Vol. 14, No. 4, pp. 327~334.

Mercer, A. and Thompson, H., 1975b, "The Purging Flow in Inclined Ducts," *J. Br. Nucl. Energy Soc.,* Vol. 14, No. 4, pp. 330~340.

Yang, W. J., 1989, *Handbook of Flow Visualization,* Hemisphere Publishing Corporation, New York, pp. 205~206.